A Multi Axis Space Phasor Based Current Hysteresis Controller for PWM Inverters

Vinay M. Mistry
M.Tech student
CEDT

S.P. Waikar
M.Tech Student
CEDT

K.Gopakumar
CEDT

L.Umanand
CEDT

V.T. Ranganathan
Electrical Engg.

Center for Electronics Design and Technology.
Indian Institute of Science
Bangalore- 560012
INDIA

(Tel. 91-80-3341810, FAX- 91-80- 3341683, E - Mail - kgopa@cedt.iisc.ernet.in)

ABSTRACT

In conventional three phase current hysteresis controllers, the current error along the three phase axes are independently controlled. This will result in random selection of switching vectors causing high inverter switching losses. In this paper, a space phasor based multi axis current hysteresis controller is proposed, in which the current error along the orthogonal axes (jA, jB, jC) are monitored. The current error boundary is a hexagon. The proposed control scheme can be implemented using simple look up tables. The advantages of the proposed current hysteresis controlled PWM scheme, when compared to other multi level current hysteresis controllers, is that only the adjacent vectors close to the motor back emf space phasor voltage, is only used for the inverter switching, for the entire speed range (optimum PWM switching). In the present scheme, the selection of the inverter voltage vectors for optimum PWM switching is achieved by, without any computation of the machine voltage space phasor, for the full speed range of the drive system. The proposed scheme is self adapting, as far as the motor space phasor voltage is concerned, and also maintains the controller simplicity and quick response features of a hysteresis current controller. The scheme is simulated and also experimentally verified .

1. Introduction

Conventional hysteresis current controllers with independent control in each phase has excellent dynamic performances [1]. But these type of controllers will go into limit cycle high frequency switching, at low back emf voltages. Also, the current error may reach twice the value of hysteresis band [2]. Predictive current controllers, with optimised PWM switching and with reduced switching frequencies, require complicated off line computations and complex implementation schemes [3] [4]. Other fast acting current controllers with optimum PWM requires, the position and magnitude information of the motor back emf . The back emf computation, such as based on the derivative of the high frequency current error, is also quite complex to implement [5]. Space phasor based current controllers are based on current error regulation in orthogonal co- ordinates (α, β - axes) [6].

Here multi level hysteresis controllers are used along the orthogonal axes. The appropriate switching vectors are chosen from simple look up tables, to limit the current error within the hysteresis boundary [6] [7]. These controllers have very good dynamic behaviour as well as good performance in the steady state. In such schemes, in order to limit the current error, vectors near to the machine voltage ($\underline{V_m}$ - back emf voltage space phasor) is not always selected, resulting in non - optimum PWM switching pattern [6] [7]. This will increase the number of inverter switchings in a cycle, resulting in high inverter switching losses.

In the following section, a multi axis (jA, jB, jC) space phasor based current hysteresis controller is explained. The proposed scheme selects adjacent vectors close to the machine voltage space phasor (irrespective of the machine voltage amplitude $|V_m|$ and position) , in a sector, for PWM current hysteresis control. The proposed scheme is self adapting and does not require any $\underline{V_m}$ computation and at the same time , simplicity of the controller design using analog circuits and look up table PWM vector selection, is maintained as in the case of other hysteresis controllers.

2. Space Phasor Based Multi Axis Hysteresis Current Controller

In space phasor based current hysteresis controllers, using orthogonal axes (α , β), the α - axis is placed along the A-phase coil axis and the β - axis is placed perpendicular to the A- phase coil axis (jA). In the proposed scheme, the current error space phasor $\underline{\Delta I(t)}$ ($I_{machine}$ - $I_{reference}$) is monitored along all the three orthogonal axes (jA, jB, jC), where, jA, jB, jC axes are the perpendicular axes for phase- A phase- B and phase - C axes, respectively.

$$L\frac{\underline{\Delta I(t)}}{dt} = \underline{V_k} - \underline{V_m} \qquad (1)$$

7803-3773-5/97/$10.00 © 1997 IEEE

(where, L = stator self inductance, $\underline{V}_k$ - inverter output voltage space phasors and $\underline{V}_m$ machine voltage space phasor.)[7].

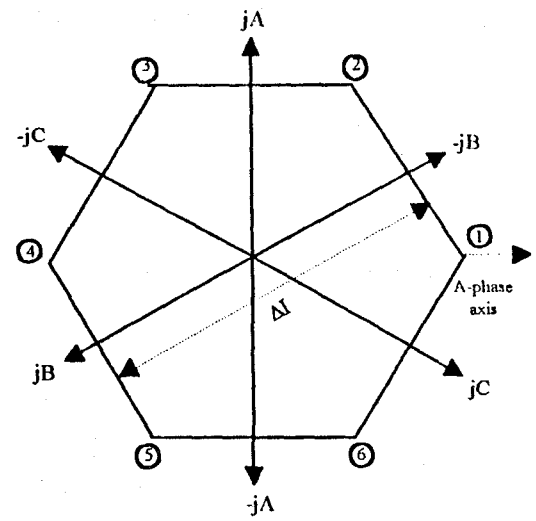

Fig. 1 Current error boundary for the multi axis current hysteresis controller

The resulting hysteresis band is a hexagon, as shown in Fig. 1. The current error monitoring along jA, jB, jC, axes can be achieved by, the current sensors along phase-A , and phase-B, and phase- C axes, and using simple analog circuits (eqn. 2) [8].

$$i_\beta(t) = \frac{\sqrt{3}}{2}\,(\,i_B(t) - i_C(t)\,) = j i_A(t) - -\alpha \text{ -along A- axis.}$$

$$i_\beta(t) = \frac{\sqrt{3}}{2}(\,i_C(t) - i_A(t)) = j i_A(t) - -\alpha \text{ - along B- axis.}$$

$$i_\beta(t) = \frac{\sqrt{3}}{2}\,(\,i_A(t) - i_B(t) = j i_C(t) - -\alpha \text{ - along C- axis. (2).}$$

In conventional independent hysteresis controllers, with out put states +1 or -1 , the current error has to reach the boundary, and should come back along the same axis, for repeated switching of the same state. This means, for the same axis, the +1 and -1 states are repeated alternately , one after the other. But in multi axis space phasor based current hysteresis controller (proposed in this paper) , the current error space phasor is controlled and it can go in any random direction within the hexagonal boundary (Fig. 1). So, some times, it is required that, repeated switching of the same controller state, in any three axes (jA, jB, jC) may occur, without going through the opposite state, in the same axis. To facilitate this, two hysteresis controllers with a small hysteresis band (δI) is placed along , each of the three axes, as shown in Fig.2. The small δI comparator level is provided, to avoid jittering of the outputs, due to noise spikes from feed back currents. Theoretically, level comparators are only required at both ends of the axis. Now the switching table formulation, for the three axes are shown in Fig. 3. In Fig. 4 the current hysteresis boundary is shown, for the proposed scheme. There is an overlap from individual axis boundary, due to δI hysteresis band. This is also taken care of in deciding the appropriate inverter switching vectors, in a

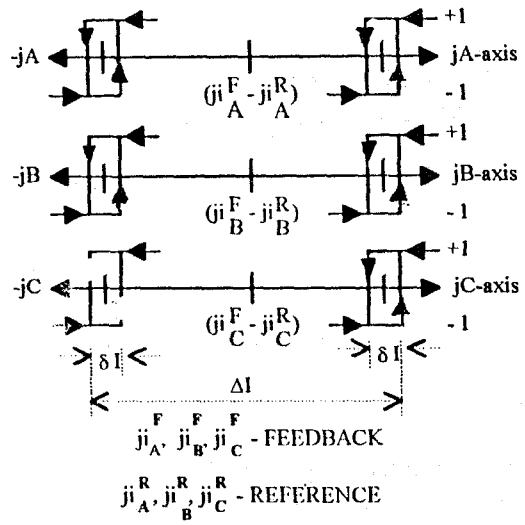

Fig. 2. Hysteresis current controllers along jA, jB, jC axes.

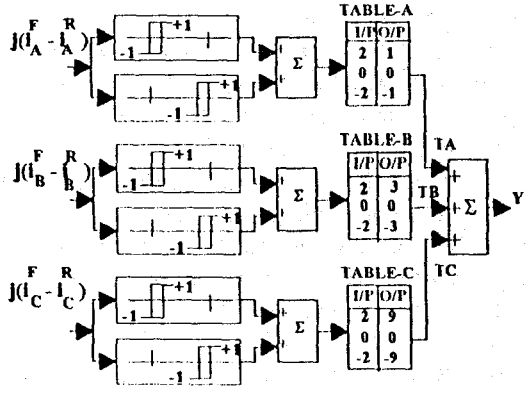

Fig. 3 Inverter switching table synthesis for multi axis current controller

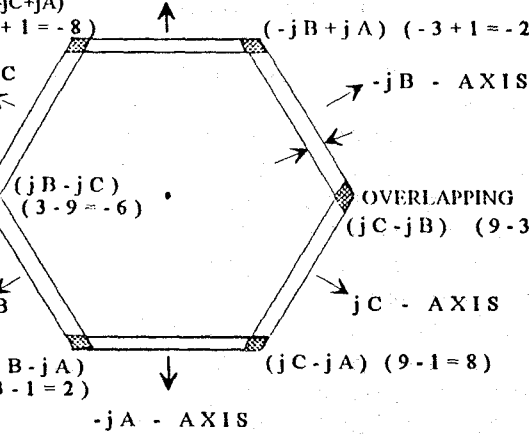

Fig. 4 Current error space phasor boundary for multiaxis controller.

sector (Table- 1.). In choosing the inverter states, fo switching in various sectors, it is taken care of that (a) only adjacent vectors , close to the machine voltage space phasor $\underline{V}_m$), is always chosen for current control, (b) among the

$Y = T_A + T_B + T_C$

<---------- Vector state from inverter ----------->

SECTOR ↑ / Y → X	-9 (-jC)	-8 (-jC+ jA)	-6 (jB- jC)	-3 (-jB)	-2 (jA+ -jB)	-1 (-jA)	0	1 (jA)	2 (-jA+ jB)	3 (jB)	6 (-jB+ jC)	8 (jC- jA)	9 (jc)
S1	1	1	1	Z	Z	2	0	Z	2	1	Z	2	2
S2	Z	Z	2	3	Z	2	0	Z	2	2	3	3	3
S3	Z	Z	Z	4	4	3	0	4	3	Z	4	3	3
S4	5	5	Z	4	5	Z	0	5	Z	Z	4	4	4
S5	6	6	6	5	5	Z	0	5	Z	6	5	Z	Z
S6	6	6	1	Z	6	1	0	6	1	1	Z	Z	Z

TABLE -1 . Vector switching look up table for the multi axis space phasor based current hysteresis controller.

↓ - indicatess the sector change and the voltage vectors involved.

Z - zero vector states (+ + +) or (- - -) [8].

0 - continue with the previous state, and no new switching action is initiated.

1,2,3,4,5,6 are the numbers for the voltage vectors $\underline{V_1}$, $\underline{V_2}$, $\underline{V_3}$, $\underline{V_4}$, $\underline{V_5}$, _

adjacent vectors, the vectors which gives the maximum current error change in the opposite direction, is chosen for the next switching [5]. Taking all this, the vector states, which gives optimum PWM vector selection, in a sector is chosen, as shown in Table- 1. In choosing the inverter vector states, the overlapping is also taken care of, by summing the outputs ($T_A + T_B + T_C$) of individual controllers (Fig. 3 and Fig. 4)

Table -1 gives the complete switching table for the proposed controller. The ' Y ' input is from the individual controllers (Fig. 3), for the appropriate voltage switching vectors. The ' X ' input to Table - 1 determines the sector, and this is achieved by three more hysteresis comparators, along the jA, jB, jC axes, with a hysteresis band $\Delta I'$, which is slightly greater than ΔI (Fig. 5). The sector selection is explained in the following section.

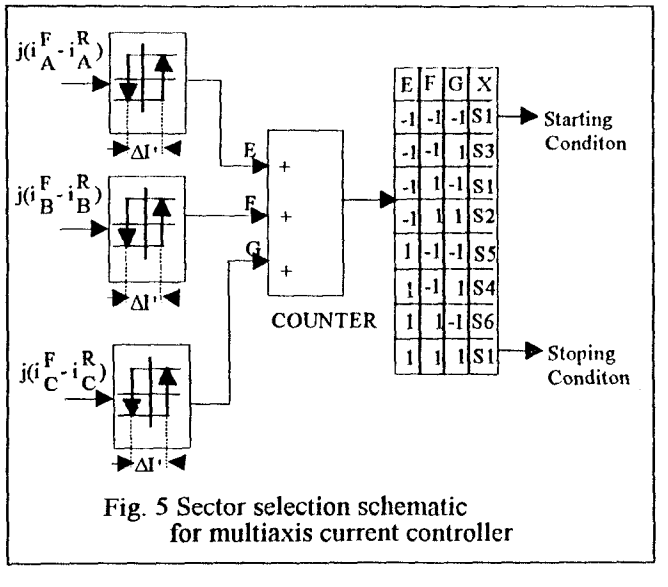

Fig. 5 Sector selection schematic for multiaxis current controller

3. Sector Selection for The Muti Axis Current Controller

The sector selection controller, proposed here is simple and self adapting, and is realised using three hysteresis comparators along the jA, jB, jC axes (Fig. 5). Fig. 6 shows

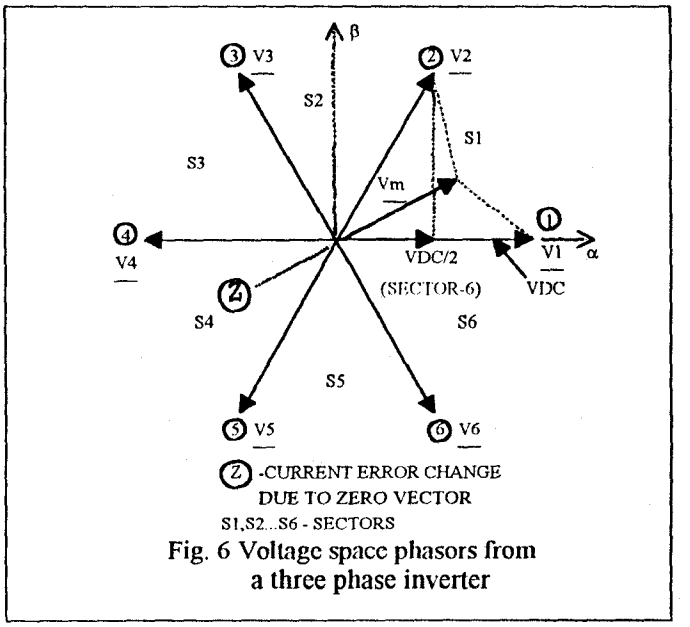

Fig. 6 Voltage space phasors from a three phase inverter

the direction of current error ($\underline{\Delta I}$) change with respect to time (dashed lines) , in sector -1 , for a $\underline{V}_m$. The ' Z ' direction (Fig. 6) is for the zero vector. Now, in sector- 1, the motor voltage space phasor $\underline{V}_m$ can only be within the triangle (including the sides AC and BC) CAB (Fig. 6) , and let the maximum amplitude $|V_m|$ can trace the side AB. When $\underline{V}_m$ is along CA (with amplitude equal to CA), the $\underline{\Delta I}$ direction is along AB, when vector - $\underline{V}_2$ is switched. Similarly, for the $\underline{V}_m$ along CB , the $\underline{\Delta I}$ direction is along

CB , when $\underline{V}_2$ is switched. In space phasor based PWM with constant switching frequency, the current error $\underline{\Delta I}$ always starts from the origin, after a sampling period [8]. In current hysteresis controlled PWM scheme the current error space phasor always starts from the hysteresis boundary, when a

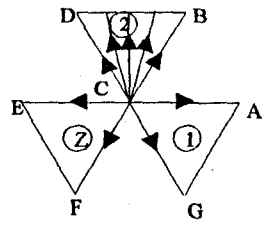

Fig.7a SECTOR - S1

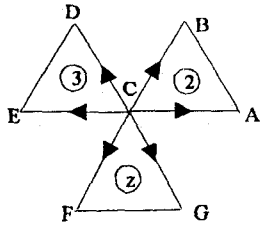

Fig. 7b SECTOR - S2

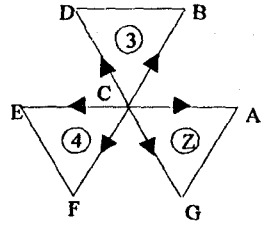

Fig.7.c SECTOR - S3

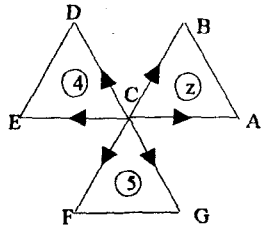

Fig. 7d SECTOR - S4

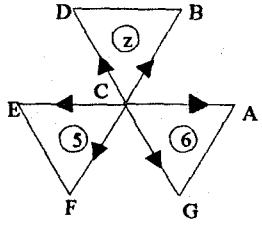

Fig. 7e SECTOR - S5

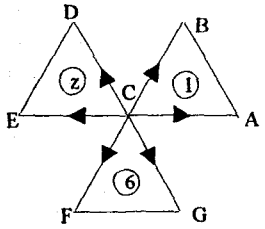

Fig. 7f SECTOR - S6

Fig.7 Current error ($\underline{\Delta}$ I(t)) direction boundaries in all the six sectors

new voltage vector is switched. Now for the proposed hexagonal hysteresis boundary , all possible current error space phasor directions, in sector- 1, when $\underline{V}_2$ is switched, will be parallel to the lines starting from the origin, shown in the triangle CBD (including the sides CD and CB) (Fig. 7a). Similarly the triangular boundary for the $\underline{\Delta I}$ direction , in sector -1, when $\underline{V}_1$ and the zero vector (Z) are switched,

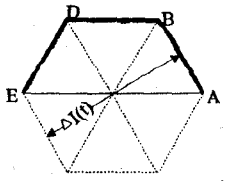

Fig. 8a
Hexagonal boundary limit for ($\underline{\Delta}$I(t)) in sector -1 for $\underline{V2}$ vector switching

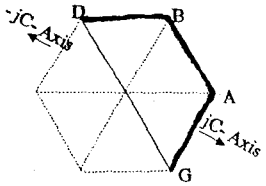

Fig. 8b
Hexagonal boundary limit for ($\underline{\Delta}$I(t)) in sector -2 for $\underline{V2}$ vector switching

are also shown in Fig.7a.

The current error phasor ($\underline{\Delta I}(t)$) direction boundary, in all the sectors , for appropriate voltage vector switching, for optimum PWM switching, is presented in Fig. 7. In the proposed hexagonal hysteresis boundary, the current error phasor starts from a hysteresis boundary point, and follows parallel to one of the direction lines, shown by the triangular direction boundaries in Fig. 7, depending on the voltage vector and the sector, till it reaches the corresponding hexagonal boundary. For example, when the voltage vector - $\underline{V}_2$ is switched , the current error phasor ($\underline{\Delta I}(t)$) , starts from a hexagonal boundary and follows any one of the directions within the direction boundary (Fig.7a.) CD and CB till it reaches the other side. Now drawing all parallel lines to CD and CB, and also to lines within the triangular direction boundary CD and CB, the hexagonal boundary region along which only, the current error phasor hits the hysteresis boundary, in sector- 1, for vector $\underline{V}_2$ switching will be obtained(Fig. 8a.). This region is for any possible $\underline{V}_m$ in sector- 1, when $\underline{V}_2$ is switched. Similarly the boundary region for $\underline{V}_2$ in sector- 2 is shown in Fig. 8b.

Let $\underline{V}_m$ phasor traces a circular trajectory, with a uniform velocity (synchronous frequency), in the anti clock wise direction. In sector- 1, as $\underline{V}_m$ moves closer to the vector $\underline{V}_2$

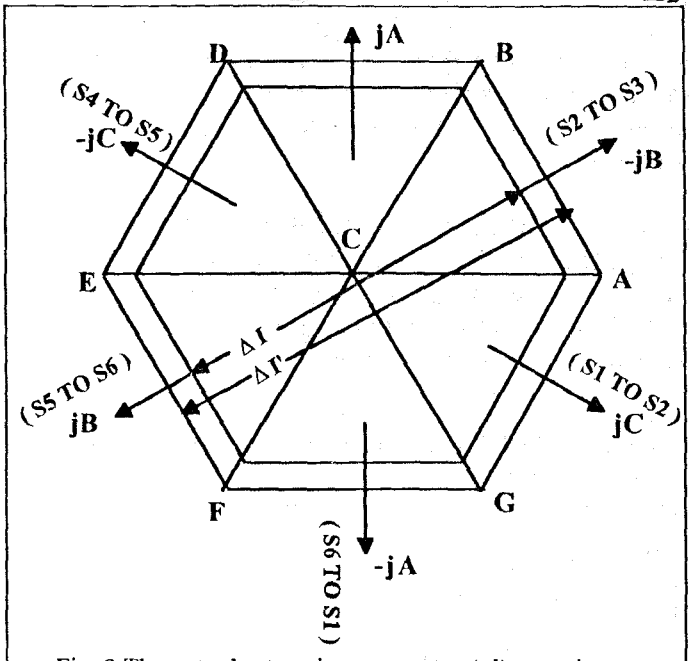

Fig. 9 The outer hysteresis comparator (ΔI') crossing along the jA, jB, jC axes, showing the corresponding sector change.

axis (Fig. 9) , the change with respect to time, for the component of the current error phasor ($\underline{\Delta I}(t)$), will be maximum along ' -jB ' axis, when $\underline{V}_2$ is switched (Fig.9. and Table.1). For the same vector position, when the zero vector is switched (in sector - 1), the maximum current error change will be along ' -jA' axis (Table- 1 and fig. 9). When $\underline{V}_m$ is along $\underline{V}_2$ axis ,the $\underline{\Delta I}(t)$ variation is parallel to the hexagonal boundary AG (Fig. 8b.), and the rate of change of

current error phasor component along 'jC' axis (FIG. 8b) is zero (sector -1). Now as $\underline{V}_m$ moves to sector- 2, the current error phasor $\underline{\Delta I}(t)$ component along jC axis increases, for the $\underline{V}_2$ and zero vector (Z) switching , and it crosses the inner hysteresis limit ΔI (along jC axis) cutting the hexagonal boundary AG (Fig. 8b). According to Table-1, the vector switching, for jC axis limit crossing is again the voltage vector $\underline{V}_2$, for sector- 1. So the current error again continues to increases along jC axis (now $\underline{V}_m$ is in sector- 2 and switching vector selection is still from sector - 1) and finally crosses the outer $\Delta I'$ boundary (Fig. 9), changing the sector selection from sector- 1 to sector -2 (Fig.5 and Fig.9). The inverter voltage vector variation, during the sector change is marked by an arrow in Table- 1. The outer hysteresis band $\Delta I'$ crossing axis, for each sector change can be found out, and are shown in Fig.9. The corresponding look up table for the sector information, is shown in Fig.5. During transition of $\underline{V}_m$ to the next sector, the current error component along one of the three axes (jA, jB, jC) crosses the outer hexagonal boundary, for every sector change (Fig.9). This transition is detected and the sector selection is changed accordingly (Fig.5).

The proposed scheme is simulated , using SIMULINK simulation package, for an induction motor drive [9]. The motor parameter used are shown in appendix- 1. The simulation is carried out for lower speed operation, for a comparative study with that of three level hysteresis current controllers [6] [7]. The voltage wave form obtained, for the proposed scheme is shown in Fig. 10 and the corresponding inverter vector states (0,1,2,3,4,5,6) are plotted and is shown in Fig. 11. The lower speed operation, for the proposed scheme shows that only adjacent vectors close to the motor space phasor voltage $\underline{V}_m$ is always chosen , in a sector (unlike in other multi level hysteresis controllers [6] [7]).

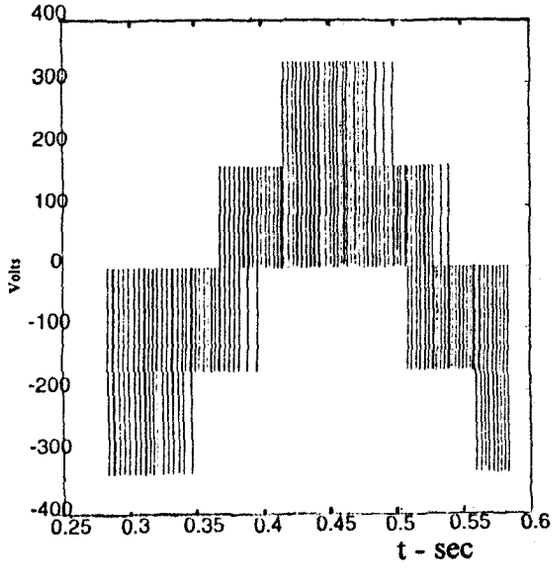

Fig. 10 The motor phase voltage waveform (multi axis space phasor based current hysteresis controller). $f = 5Hz$.

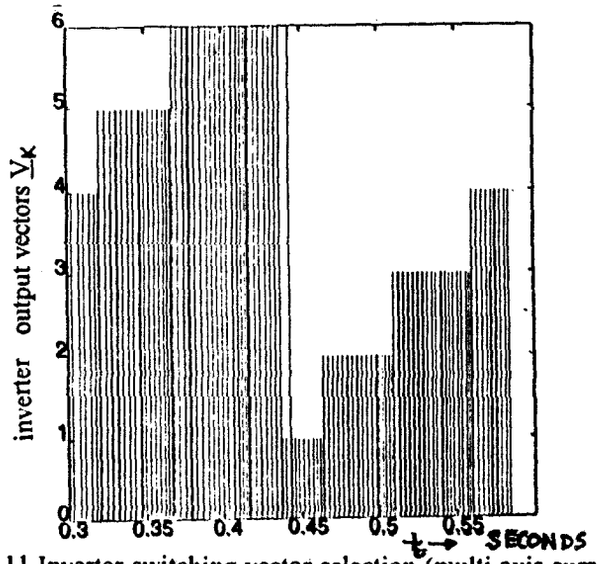

Fig. 11 Inverter switching vector selection (multi axis current hysteresis controller).

The envelope of the motor phase voltage waveform is that of a six step waveform [8]. The sector change is smooth and only one inverter leg is switched during a sector change. Unlike the other multi level current hysteresis controller schemes ([6] [7]), there is no cross over to adjacent sectors, for switching vector selection , when the machine voltage is in a particular sector, for the proposed scheme. The motor phase current waveform for the proposed scheme is shown in Fig. 12. The present scheme is also simulated in the upper frequency range, and the motor phase voltage waveform obtained from the proposed scheme is shown in Fig.13. Both the voltage waveforms (Fig 11 and Fig.13) confirms that only adjacent vectors forming a sector, close to the machine voltage space phasor in that sector, is only chosen for current control (optimum PWM operation). The resulting hexagonal current error boundary obtained, for the proposed scheme, is shown in Fig. 14.

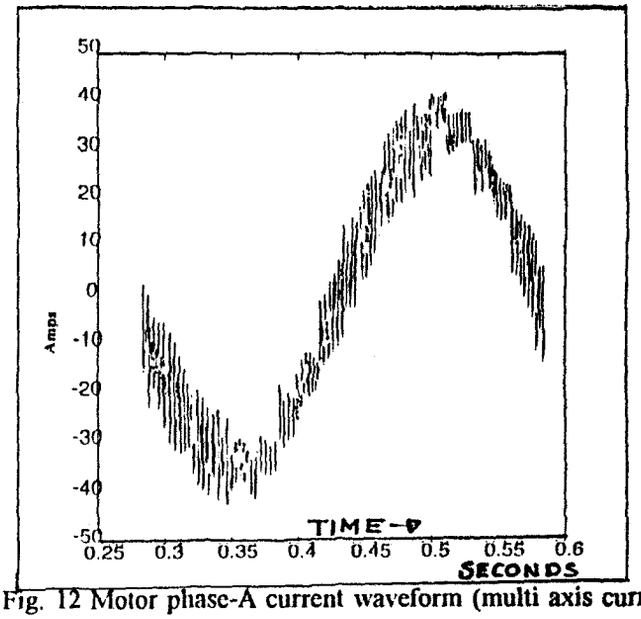

Fig. 12 Motor phase-A current waveform (multi axis current hysteresis controller).

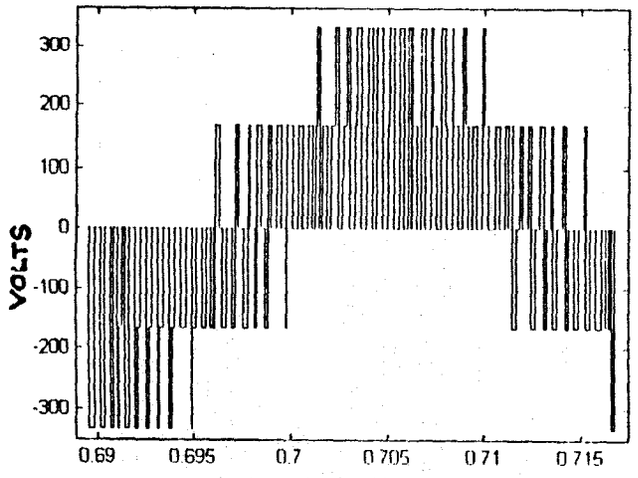

Fig. 13 Phase-A voltage waveform (multi axis current hysteresis controller) f = 33Hz.

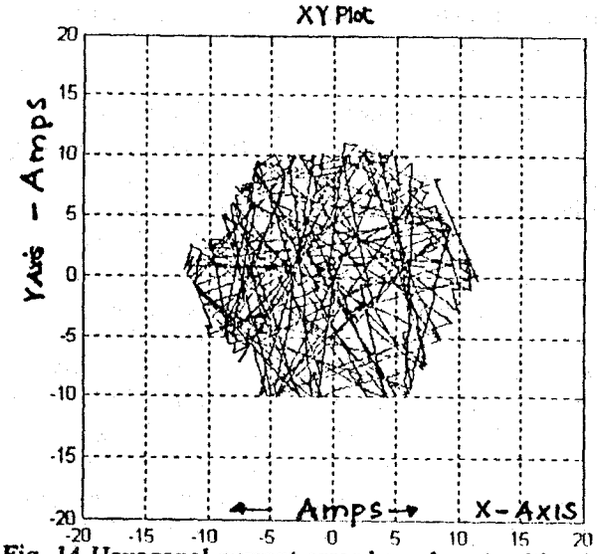

Fig. 14 Hexagonal current error boundary (multi axis current hysteresis controller).

4. Experimental Results

The scheme is experimentally verified on a 5HP induction motor drive (no load operation), using current sensors and simple look up table hysteresis levels for the inverter switching (Table.1). The phase voltage and current waveforms for a 16Hz output frequency are shown in Fig. 15. The output phase voltage and current waveform for a 33Hz out put frequency are shown in Fig.16. Both the waveforms confirm that, the inverter output voltage space phasors, forming a sector in which the machine voltage space phasor is located, are only always selected for the PWM operation. The sector change is also found to be smooth. For higher speed of operation, the proposed scheme is found to change slowly to six - step operation. The six step out put wave forms obtained from the proposed PWM strategy are shown in Fig. 17. The α , β components of the output currents are plotted in X - Y mode and the output current space phasor thus obtained is shown in Fig. 18. The hexagonal current error boundary proposed for the present scheme is clearly visible in Fig.18. The frequency spectrum of the phase voltage and current (Fig.19 and Fig. 20) waveforms do not show any

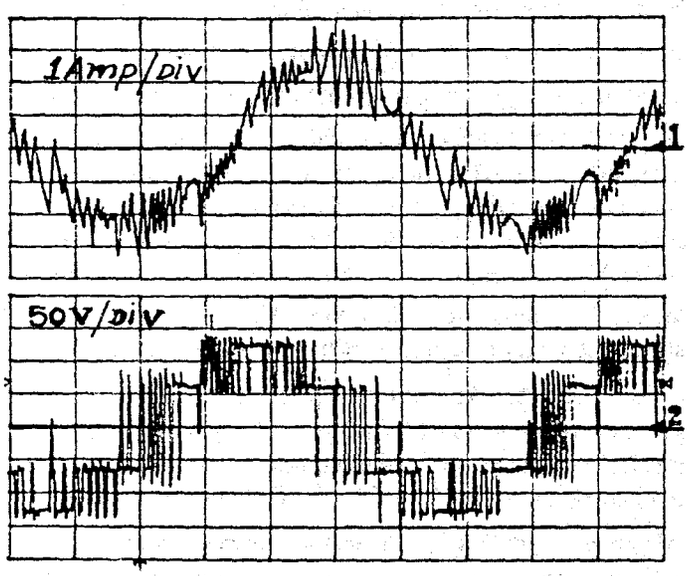

Fig.15 . Phase voltage and current : X-10 ms/div (No load)

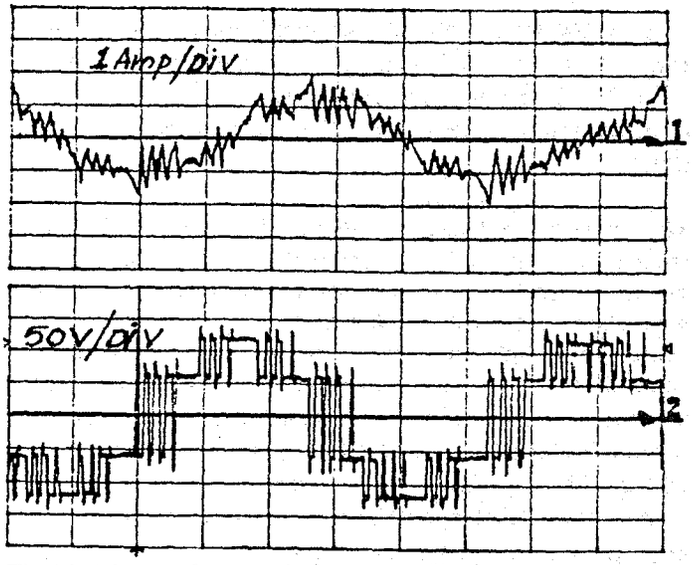

Fig.16 . Phase voltage and current : X-5 ms/ div (No load)

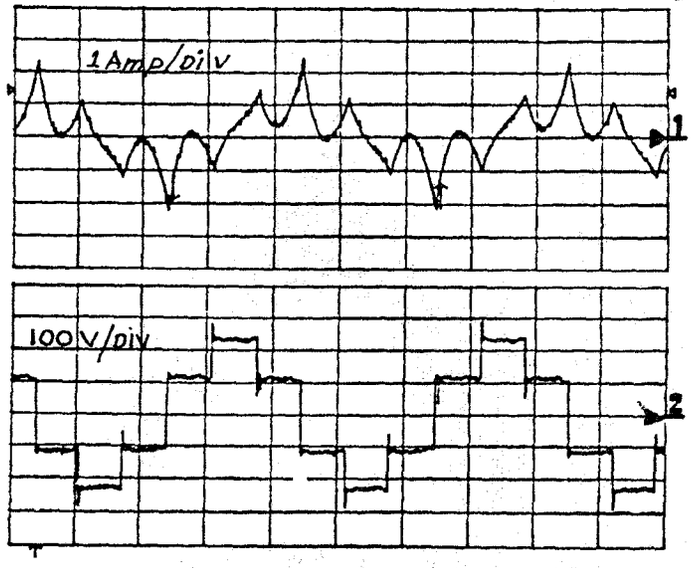

Fig. 17 Phase voltage and current for Six - step operation : X- axis 5ms/div. (50 Hz output frequency, No load).

high amplitude harmonic peaks, as in the case of other

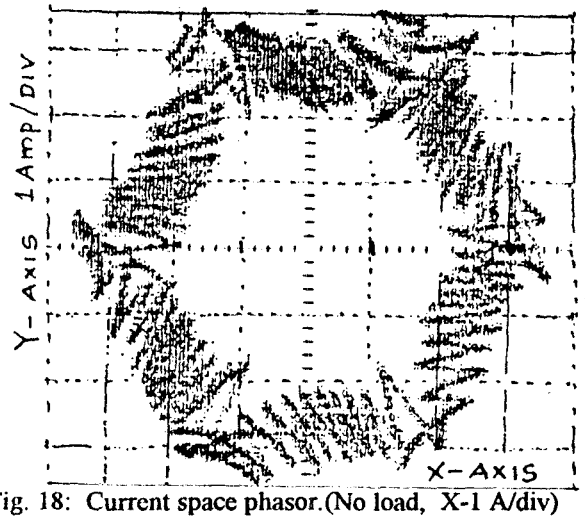

Fig. 18: Current space phasor.(No load, X-1 A/div)

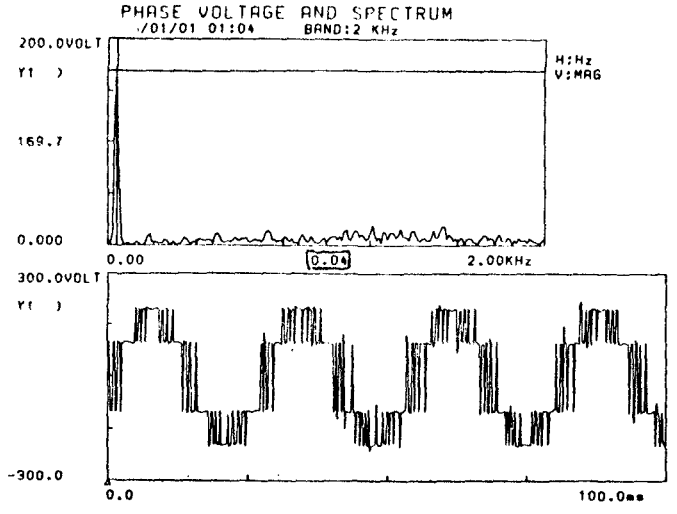

Fig 19: Phase voltage and spectrum (f = 40 Hz)

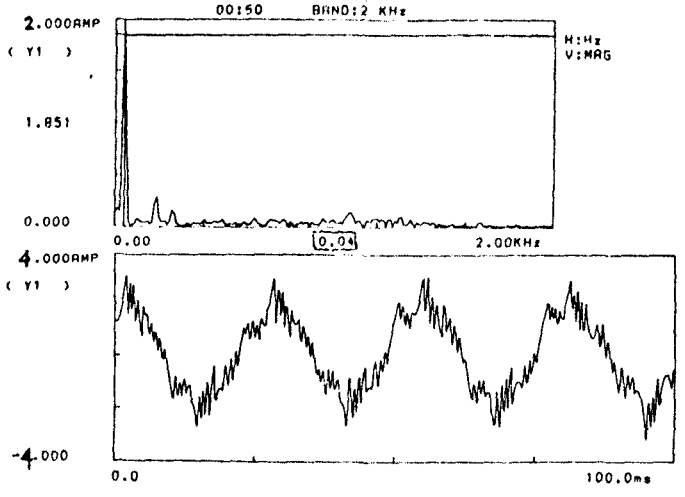

Fig 20 : Phase current and spectrum (f = 40 Hz, No load)

constant frequency (carrier based) PWM techniques. A low amplitude spread spectrum harmonic profile is observed for the PWM outputs, for the proposed study. This is because of the absence of any costant carrier frequency based switching and the proposed scheme works with a switching frequency variation (confined to a sector and is repeated in all the six sectors uniformly, depending on the machine back emf space phasor and the hysteresis bands).

5. Conclusion

A simple multi axis current controller is proposed in this paper. The current controller is based on hysteresis comparators and simple look up tables for the inverter switching. Only adjacent vectors are always chosen, for any possible value of motor space phasor voltage ($\underline{V}m$) , in a sector, for variable speed operation. Thus the number of inverter switchings , for a cycle of operation, is always less when compared to any other current hysteresis controllers. The sector selection is simple , and is achieved by a set of three hysteresis comparators along the three orthogonal axes (jA, jB, jC). The motor back emf computation is not required ($\underline{V}m$), and the proposed scheme is self adapting, for any possible amplitude and position of the machine voltage space phasor, for optimum PWM switching. All the advantages of the conventional current hysteresis controllers, as regards to quick response and simple implementation, are retained in the proposed scheme.

6. References

[1] W. Mc Murray : Modulation of the chopping frequency in DC choppers and PWM inverters having current hysteresis controllers. IEEE, Conf., PESC, pp.295-299, 1983.

[2] Brod. D.M., Novotny D.W : Current control of VSI-PWM inverters, IEEE, Trans., ind., appl.., Vol. IA-21, No.4, pp 769-775, july/aug., 1985.

[3] Holtz, J, Stadtfeld, S : A predictive controller for the stator current vector of AC machines fed from a switched voltage source, IPEC- conf., Tokyo, 1983.

[4] Holtz, J, Stadtfeld, S : A PWM inverter drive system with on - line optimised pulse patterns, EPE , conf., pp. 3.21-3.25, 1985.

[5] A. Nabae., S.Ogasawara., H. Akagi : A novel control scheme for current controlled PWM inverters, IEEE, Trans., ind., appl., Vol.IA- 22 , No. 4, pp.697 - 701., july/aug., 1986.

[6] Kazmierkowski, M.P., Dzieniakowski, M.A., Sulkowski, W : Novel space phasor based current controller for PWM inverters, IEEE, Trans., Power Electronics, Vol.6, No.1, pp. 158 - 164, jan. 1991.

[7] A. Ackva, H. Reinold, R. Olesinski : A simple and self adapting high performance current control scheme for three phase voltage source inverters, IEEE, conf., IAS, pp.435-442, 1992.

[8] H. H Van der Broeck, H. ch. Skudelny, G. Stanke : Analysis and realisation of a pulse width modulator based on voltage space vectors, IEEE, IAS, conf., pp. 244 - 251, 1986.

[9] SIMULINK, User's Guide - for use with Microsoft Windows, Mathworks Inc., 1992.

Appendix

Induction motor drive specifications (for simulation study)

3 phase, 400Vrms, 50Hz, 4 pole.

$R_s = 0.19\Omega$, $R_r = 0.125\Omega$, $M = 0.0369H$, $L_{ss} = 0.03851H$, $L_{rr} = 0.03756H$ Nominal drive torque is 10 N.m, $J = 0.1$, $B = 0.01$, $\Delta I = 20Amp$, $\Delta I' = 22Amp$.